Formation of silicate nanoscrolls through solvothermal treatment of layered octosilicate intercalated with organoammonium ions

Journal Name

ARTICLE

Formation of silicate nanoscrolls through solvothermal treatment of layered octosilicate intercalated with organoammonium ions

Yusuke Asakura,[a] Megumi Sugihara,[b] Takeru Hirohashi,[b] Aya Torimoto,[b] Takuya Matsumoto,[b] Masakazu Koike,[b] Yoshiyuki Kuroda,[c] Hiroaki Wada,[b] Atsushi Shimojima[b] and Kazuyuki Kuroda*[b,d]

We report silicate nanoscrolls composed of only SiO_4 tetrahedra with crystalline walls for the first time in this study. The procedure consists of the intercalation of layered octosilicate with dioctadecyldimethylammonium bromide ((C_{18})$_2$DMABr) and the subsequent solvothermal treatment of the intercalated material in heptane. The walls of the obtained nanoscrolls are crystalline, which originates from layer crystallinity in the pristine silicate. The direction of rolling up is fixed at the *a*- or *b*-axis of the silicate based on the electron diffraction patterns of the nanoscrolls. Desorption of (C_{18})$_2$DMABr, which is present in addition to (C_{18})$_2$DMA cations, from the interlayer during solvothermal treatment is likely related to the nanoscrolling process. Although the yield of nanoscrolls is low, these findings will lead to the re-estimation of many layered silicates intercalated with long-chain alkylammonium compounds as precursors for silicate nanoscrolls with crystalline walls.

Introduction

Nanoscrolls with one-dimensional (1D) nanostructures, formed by the exfoliation and rolling up of layered inorganic materials, are attracting much research interest due to their unique architecture and potential applications.[1] They contain two kinds of nanospaces, tubular nanopores and variable interlayers within the walls of the tubular structures. The variable interlayers are unique in nanoscrolls, being in contrast to concentric-type multi-wall nanotubes. Nanoscrolls have been obtained from various layered materials, including graphene,[2] hexagonal boron nitride,[3] layered sulfides/selenides,[4] layered hexaniobates,[5] layered titanate,[1a] layered manganese oxide,[1a] layered tantalates/titanotantalates,[6] layered vanadates,[7] chrysotile (layered magnesium silicate),[8] hydrated halloysite and organically intercalated kaolinite (both are layered aluminosilicates),[9] and layered (double) hydroxides.[10] Various applications of nanoscrolls have been studied as catalysts,[5a,11] electrochemical devices, etc.[12] The surface-related functions including (photo)catalysis of nanoscrolls are expected to be useful because of larger specific surface area. Nanosheets

possibly tend to aggregate to significantly lose accessible surfaces, while the interlayer surfaces in nanoscrolls can be utilized after aggregation.[5b,9d] As the properties of nanoscrolls depend on nanoscroll structure and composition, increasing the number of available compositions is important for further development of materials chemistry on nanoscrolls.

To generate nanoscrolls from layered materials, the following requirements should be satisfied. i) A decrease in the interactions between neighboring layers and ii) asymmetric factors within a layer. With regard to the first requirement i), the interactions between neighboring layers should be decreased for peeling to occur. The requirement ii) can induce tensile forces within the layer and hence the layer can scroll. The asymmetry of a single layer is directly reflected in the asymmetric layer structure itself[5,9] and/or environmental differences between the outer and inner surfaces of the outermost layers.[1a,2-4,6-7,10]

Naturally occurring hydrated halloysite is well known to possess nanoscrolls arising from the asymmetric nature of 1:1 type clay mineral composed of tetrahedral silicate layers and octahedral aluminate layers. The nanoscrolling is caused by the interlayer water, relaxing the structural tension.[13] Kaolinite, typical 1:1 type clay mineral, can be converted into nanoscrolls by relaxing the same tension by intercalation of large organic compounds like long-chain alkyltrimethylammonium chloride.[9d] Some layered materials with symmetric layers cannot be converted into nanoscrolls, implying that the simultaneous fulfilment of the above-stated two requirements is very difficult. Therefore, to increase the variety of nanoscrolls available, new methods are needed.

Thus far, there have been no reports on the conversion of synthetic layered silicates into nanoscrolls. They possess

a. *Institute of Multidisciplinary Research for Advanced Materials (IMRAM), Tohoku University, 2-1-1 Katahira, Aoba-ku, Sendai 980-8577, Japan.*
b. *Department of Applied Chemistry, Faculty of Science and Engineering, Waseda University, 3-4-1 Ohkubo, Shinjuku-ku, Tokyo 169-8555, Japan.*
c. *Green Hydrogen Research Center, Yokohama National University, 79-5 Tokiwadai, Hodogaya-ku, Yokohama 240-8501, Japan.*
d. *Kagami Memorial Research Institute for Materials Science and Technology, Waseda University, 2-8-26 Nishiwaseda, Shinjuku-ku, Tokyo 169-0051, Japan.*
† Electronic Supplementary Information (ESI) available: Elemental analysis, ^{29}Si MAS NMR spectra, SEM images, TEM images, and ED pattern of the samples. See DOI: 10.1039/x0xx00000x

crystalline layers composed mainly of SiO_4 tetrahedra and exchangeable cations in the interlayer spaces.[14] The most characteristic aspect of layered silicates is the presence of Si–OH groups regularly arranged on the interlayer surfaces due to layer crystallinity. Such Si–OH groups can participate in covalent reactions[15] including inter-[16] or intra-layer condensation,[17] silylation,[18] and esterification.[19] When nanosheets scroll to form nanoscrolls, channel-like nanopores are generated in the center part of the obtained nanoscrolls. Therefore, nanoscrolls derived from layered silicates can be regarded as nanoporous silica with crystalline walls and regularly arranged Si–OH groups on the surfaces of inner and outer tubular nanosheets. Such unique nanoporous silica is very promising, because the surfaces of pore walls can be modified in an ordered manner using the regularly arranged Si–OH groups. Such regular arrangement is useful for determining the distance between immobilized functional groups. This control can contribute to a deeper understanding of the mechanisms of catalysis and chemical adsorption by defining the reactive and adsorption sites. However, nanoscrolls composed of pure silica have not been reported so far to the best of our knowledge, probably because almost all layered silicates contain symmetric layers, suggesting that they cannot be easily converted into exfoliated/delaminated nanosheets by decreasing interactions between neighboring layers. If a process can be designed to fabricate silicate nanoscrolls from layered silicates, such a method can be used to increase the variety of nanoscrolls available. Further, this method might open up a new avenue to produce nanoscrolls from layered materials.
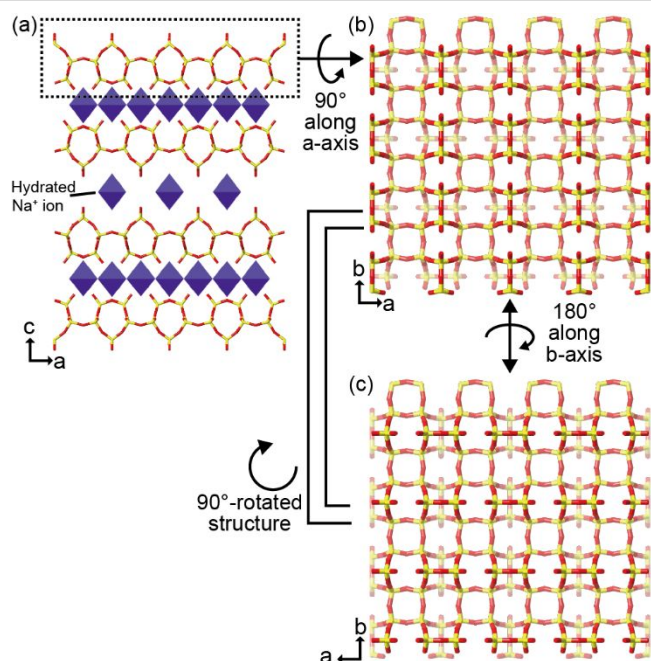

Fig. 1 (a) Crystal structure of layered octosilicate, (b) perpendicular view of a layer in the layered octosilicate, and (c) reverse side view of the layer in (b). Please note that the directions of faint and strong lines are different by 90° between (b) and (c).

We focused on the delamination of a layered octosilicate[20] (Na-Oct: $Na_8[Si_{32}O_{64}(OH)_8 \cdot 32H_2O]$, so called RUB-18,[21] the structure and crystallographic data are shown in Fig. 1a and ESI, respectively) for the synthesis of silicate nanoscrolls. The method for delamination fulfills one requirement for the formation of nanoscrolls, i.e., a decrease in interlayer interactions. Hence, we reinvestigated the procedure in order to simultaneously fulfill the two requirements. From another point of view, Na-Oct is worthy of being investigated for the formation of nanoscrolls because it has unique layers. In one layer, the 90°-rotated structure of the obverse side is equivalent to the structure of the reverse side (Fig. 1b and c). Such a relationship between the obverse and reverse sides should prevent scrolling, because the structural relationship makes it difficult to determine a direction for easy scrolling. Therefore, if Na-Oct can be converted into nanoscrolls through a sophisticated procedure, the procedure can be applied to other layered materials from which nanoscrolls could not previously be produced.

Scheme 1. Formation of silicate nanoscrolls through (i) intercalation of layered octosilicate with $(C_{18})_2$DMABr and (ii) subsequent solvothermal treatment with heptane

Our previously reported method for the delamination of layered octosilicate consisted of two steps, i.e., intercalation of layered octosilicate with didecyldimethylammonium bromide, followed by sonication.[20] In the present study, we found that the solvothermal treatment of layered octosilicate intercalated with dioctadecyldimethylammonium cations leads to the formation of nanoscrolls. The experimental procedure is shown in Scheme 1. Firstly, layered octosilicate (Na-Oct) is intercalated with dioctadecyldimethylammonium bromide $((C_{18})_2$DMABr). Later, $(C_{18})_2$DMA-Oct is treated solvothermally in heptane at 120 °C with stirring for 1 d. Further, we also discuss the proposed mechanism for nanoscrolling.

Experimental

Materials.

SiO_2 and NaOH were purchased from Aldrich and Wako Pure Chemical. Ind., Ltd., respectively, and used without further purification for synthesis of layered octosilicate. Dioctadecyldimethylammonium bromide $((C_{18})_2$DMABr) and heptane were purchased from Tokyo Chem. Ind. Co., Ltd. Layered octosilicate (Na-Oct) was prepared according to our previous literature.[18h]

Intercalation of layered silicate with $(C_{18})_2$DMABr.

$(C_{18})_2$DMABr (7.89 g) was added to water (500 mL) to obtain a dispersed solution. The prepared solution was not transparent,

which means that some amounts of $(C_{18})_2DMABr$ did not dissolve in the solution. To this solution (149 g), the layered octosilicate (0.81 g) was added. The mixture was then stirred at 80 °C for 1 h. At the end of the reaction period, the mixed solution was centrifuged twice to remove the supernatant. The resultant product was washed twice with ethanol for 10 min and dried under reduced pressure. The obtained sample was denoted as $(C_{18})_2DMA$-Oct.

Solvothermal treatment of $(C_{18})_2DMA$-Oct in heptane.

$(C_{18})_2DMA$-Oct (10 mg) was added to heptane (5 mL) and the mixture was treated solvothermally in a 100 mL Teflon-sealed autoclave at 120 °C for 1 d with stirring at 300 rpm. The product was denoted as solvo-$(C_{18})_2DMA$-Oct.†† The treated mixture itself (before separation) was used for scanning electron microscopy (SEM) and transmission electron microscopy (TEM). The sample obtained after centrifugation and drying was analyzed by powder X-ray diffraction (XRD), thermogravimetry, elemental analysis, and solid-state ^{29}Si magic angle spinning-nuclear magnetic resonance (^{29}Si MAS NMR).

Characterization.

The XRD patterns were generated on a Rigaku Ultima-III powder diffractometer (Cu Kα, λ = 0.15418 nm, 40 kV, 40 mA) with parallel beam geometry. The SEM images were recorded on a Hitachi S-4500S microscope at an accelerating voltage of 5 kV; the samples were observed after coating with Pt and Pd metals. The samples dispersed in heptane were dropped on carbon-reinforced micro grids and dried. Powder samples were adhered on carbon tapes for SEM observations. TEM images and selected area electron diffraction (SAED) patterns were obtained on a JEOL JEM-2010 microscope at an accelerating voltage of 200 kV. The samples dispersed in heptane were dropped on carbon-reinforced micro grids and dried for TEM observations. The amount of carbon, hydrogen, and nitrogen in the samples was determined by CHN analysis (Perkin-Elmer, 2400 Series II). The amounts of Na and Si were determined by inductively coupled plasma emission spectrometry (Agilent Technologies, Agilent 5100). The samples were pre-treated by melting with $Li_2B_4O_7$. Thermogravimetry was conducted on a Rigaku Thermo Plus EVO 2 TG8121 instrument in a dry-air flow (200 mL·min^{-1}). The residual amount obtained after thermogravimetric analysis up to 900 °C was regarded as the amount of silica in the samples. During thermogravimetric analysis, the samples were heated at a rate of 10 °C·min^{-1} up to 900 °C. Solid-state ^{29}Si MAS NMR spectra were recorded on a JEOL ECX-400 spectrometer at a resonance frequency of 78.65 MHz with a 90° pulse and recycle delay of 400 s using a 4 mm zirconia rotor spinning at 6.1 kHz.

Results and Discussion

The powder XRD pattern of $(C_{18})_2DMA$-Oct shows that its basal spacing (4.3 nm) was higher than that of Na-Oct (1.1 nm), while that of solvo-$(C_{18})_2DMA$-Oct (3.7 nm) decreased

when compared to $(C_{18})_2DMA$-Oct (4.3 nm). In addition, the peak attributed to the (400) plane of Na-Oct appeared at around 2θ = 49° due to the layer (in plane) crystallinity, being retained after intercalation and the subsequent solvothermal treatment (Fig. 2). Chemical analysis of $(C_{18})_2DMA$-Oct (Table S1) shows a large decrease in the concentration of interlayer Na cations and the insertion of $(C_{18})_2DMA$ cations in the interlayer. On the other hand, chemical analysis of solvo-$(C_{18})_2DMA$-Oct (Table S1) shows the partial desorption of interlayer ammonium cations from the interlayer. The Q^3/Q^4 ratios (Q^n = $Si(OSi)_n(O^-/OH)_{4-n}$) of $(C_{18})_2DMA$-Oct (1.1) and solvo-$(C_{18})_2DMA$-Oct (1.2) in the solid-state ^{29}Si MAS NMR spectra are similar to that of Na-Oct (Fig. S1), though the observed values are slightly higher than the value of the ideal structure of layered octosilicate (1.0). The NMR data suggest that the layer structure did not collapse. These XRD and ^{29}Si MAS NMR results reflected the whole sample, including not only bulk region but also nanoscrolls. Thus, the XRD and NMR measurements were used to prove the retention of the original silicate structure.
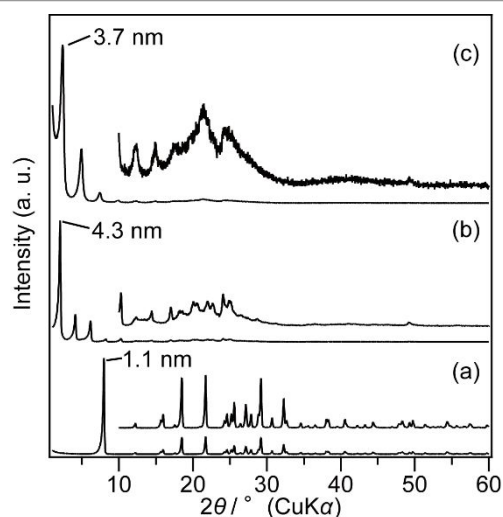

Fig. 2 XRD patterns of (a) Na-Oct, (b) $(C_{18})_2DMA$-Oct, and (c) solvo-$(C_{18})_2DMA$-Oct.
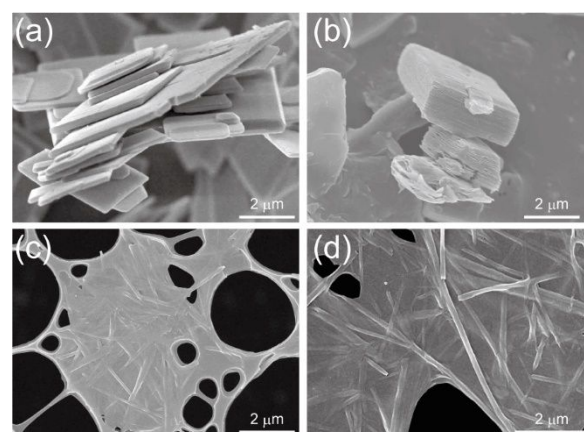

Fig. 3 SEM images of (a) Na-Oct, (b) $(C_{18})_2DMA$-Oct, and (c and d) solvo-$(C_{18})_2DMA$-Oct.

The SEM image of $(C_{18})_2DMA$-Oct indicates a plate-like morphology with slightly defective sites (Fig. S2); it is

essentially similar to that of Na-Oct (Figs. 3a and b). It should be noted that the average thickness of $(C_{18})_2$DMA-Oct (*ca.* 0.9 μm) is four times greater than that of Na-Oct (*ca.* 0.2 μm) and the difference is consistent with that between their basal spacings.

The SEM images of solvo-$(C_{18})_2$DMA-Oct (Figs. 3c and d) show 1D rod-like particles, though plate-like particles and delaminated particles (Fig. S3) could also be observed. The length of the obtained rod-like particles is 1 to 6 μm. The TEM images of solvo-$(C_{18})_2$DMA-Oct (Fig. 4) show that each rod-like particle possesses a tubular pore inside the rod-like particle and a layer-like structure in the wall. The inside tubular pore size of the observed rods was in the range of 40 to 60 nm, indicating that the obtained tubes possessed pores in the range of boundary zone between meso- and macro-pores. Though the quality of the TEM images (Fig. 4c) are not clear enough to correctly count the number of stacking layers, the number of layers in the lower wall should be equal to that in the upper wall, or one layer larger or smaller.

The original size of a flat single nanosheet before scrolling is calculated from the inner diameter of a nanoscroll (D = 46.6 nm) and the distance between the stacking layers in the wall (d = 3.2 nm). The two values are obtained from a typical nanoscroll. In this calculation, we hypothesized that the nanoscroll is a multiwall nanotube, meaning that the cross section of the hypothesized tube forms thirteen concentric circles. Based on the two equations shown in the ESI, the original size of the nanosheet is calculated to be 2.1 μm. The value is consistent with the edge length of the platy crystal, suggesting that the scroll is composed of a layer. It should be noted that the size of the corresponding original nanosheet before scrolling is not always the same, with the average being 1.9 μm.
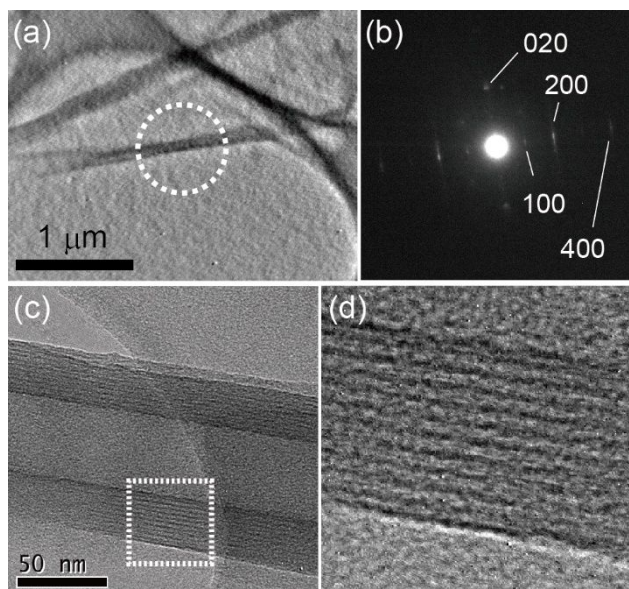
The ED patterns obtained from a selected nanoscroll from a very thin sample of solvo-$(C_{18})_2$DMA-Oct (Fig. 4b) are similar to the ED patterns of pristine Na-Oct with four-fold symmetry (Fig. S4), thus indicating that the walls of nanoscrolls are crystalline in nature. In addition, all the spots in the ED patterns contain streaks in the direction perpendicular to the long axis of the nanoscroll. This characteristic is typical of nanoscrolls,[22] which suggests a distortion in the crystal structure along the scrolling direction. Even if delaminated plates are contaminated in the grid, the presence of the streaks strongly suggest the formation of nanoscrolls. The scrolling direction is considered to be the *a*- or *b*-axis of the layered octosilicate (the *a*- and *b*-axes are equivalent to those of the layered octosilicate, as shown in Fig. 1). These results clearly show that silicate nanoscrolls could be obtained by the solvothermal treatment of $(C_{18})_2$DMA-Oct with heptane. Because of their tubular nanopores and wall crystallinity, these nanoscrolls can be regarded as crystalline nanoporous silica. In addition, the retention of crystal structure in the layered octosilicate results in orderly arranged Si–OH groups being available on the surfaces of the pore walls. Nanoporous silica with orderly arranged Si–OH groups on the surfaces has not been reported thus far; the obtained nanoscrolls can be applied as new supports for the orderly immobilization of functional groups, which can lead to a better understanding of catalysis and chemical adsorption.
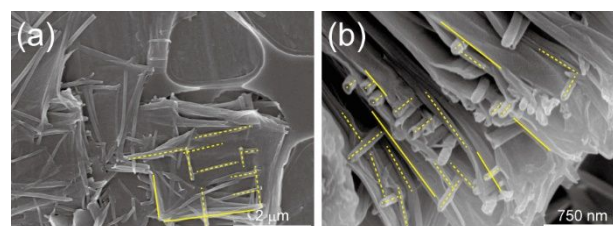

Fig. 5 SEM images of $(C_{18})_2$DMA-Oct treated solvothermally for 2 h. (a) Surface view and (b) side view of a plate particle. In the images, the solid and dashed lines indicate edges of the particles and the long axis of the nanoscrolls, respectively.
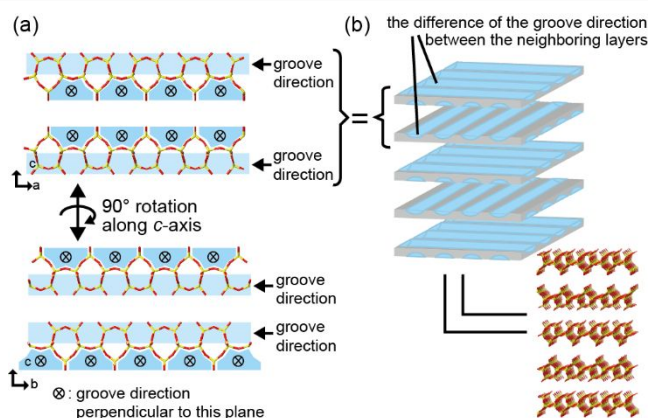
Fig. 6 (a) Relationship in the stacking sequence of Na-Oct and (b) relationship between the grooves of neighboring layers

When the solvothermal-treatment time of $(C_{18})_2$DMA-Oct is shortened from 1 d to 2 h, nanoscrolls are observed on a platy particle and even between layers, as observed in the SEM

Fig. 4 (a) TEM image of solvo-$(C_{18})_2$DMA-Oct, (b) SAED pattern of image (a), (c) high-resolution TEM image of the nanoscrolls of solvo-$(C_{18})_2$DMA-Oct, and (d) expanded view of the square area of image (d)

Scheme 2. Proposed mechanism for the formation of silicate nanoscrolls under solvothermal conditions
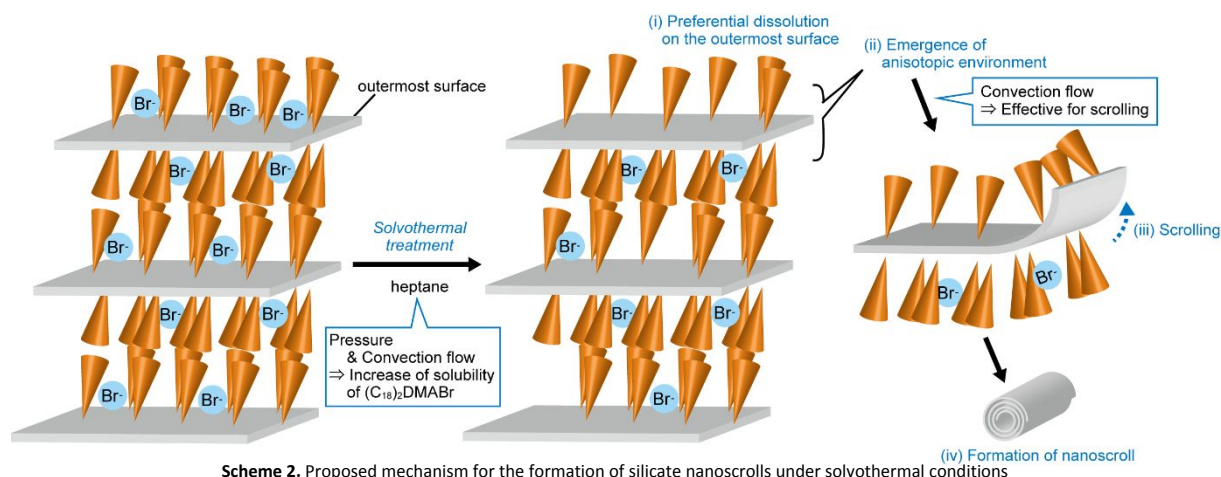
images (Figs. 5a and b, respectively). The solvothermal treatment for longer reaction time should increase the conversion ratio of pristine plates to nanoscrolls or highly delaminated plates, resulting in the lowering of the amount of nanoscrolls attached directly to the plates. As found for Figs. 5a and b, the long axis of the nanoscrolls is usually parallel to the edges of a square plate, but sometimes the nanoscrolls are orthogonal to the square plates. Orthogonal crossing is also observed in the SEM image of solvo-$(C_{18})_2$DMA-Oct obtained after solvothermal treatment for 1 d (Fig. S5). Because the edges of the square plate are parallel to the *a*- and *b*-axes of the layered octosilicate, this observation is in good agreement with the finding that the scrolling direction is along the *a*- or *b*-axis, as observed in the ED patterns.

The orthogonal crossing of nanoscrolls can be explained as follows. The layers of the octosilicate contain uniaxial grooves on both surfaces and the direction of the grooves on one side is perpendicular to those on the opposite side (Fig. 6). A layer is rotated by 90° with respect to the neighboring one, thus forming an ABAB-type stacking sequence. Accordingly, when one layer is peeled off from the outermost basal plane of a particle, the direction of the subsequently exposed grooves changes by 90°. Therefore, the perpendicular crossing of the scrolling seems to be consistent with ABAB-type stacking. The direction of scrolling is dependent on the direction of the grooves (surface structure of a layer).

As shown above, the N/Si ratio of solvo-$(C_{18})_2$DMA-Oct (0.17) is smaller than that of $(C_{18})_2$DMA-Oct (0.23) (Table S1), and the basal spacing deceased from 4.3 nm to 3.7 nm after the solvothermal reaction (Fig. 2). When $(C_{18})_2$DMA cations exist as the counter cations of anionic interlayer-surface SiO⁻, solvothermal treatment does not lead to the desorption of cations due to the absence of other exchangeable cations in the solvent used. The average Br/Si ratios of $(C_{18})_2$DMA-Oct (Br/Si = 0.07) and solvo-$(C_{18})_2$DMA-Oct (Br/Si = 0.03), as roughly estimated by the EDX analyses (Fig. S6 and Table S1), show the presence of Br⁻ in both of the samples and the decrease of $(C_{18})_2$DMABr after the solvothermal treatment. Because the Br/Si ratio of $(C_{18})_2$DMA-Oct is approximately 1/3 of the N/Si ratio, it is quite reasonable to estimate that $(C_{18})_2$DMABr salts should reside in the interlayer space and

also on the outermost surface of $(C_{18})_2$DMA-Oct. The species adsorbed on the outermost surface should be more easily desorbed than those in the interlayer species because of their lesser confined environments. Therefore, the decrease in the N/Si and Br/Si ratios can be explained by the desorption of $(C_{18})_2$DMABr salts and $(C_{18})_2$DMA cations from the interlayer space and the outermost surface of solvo-$(C_{18})_2$DMA-Oct.

The effects of 1) temperature during heating treatment, 2) autogenous high pressure in the solvothermal environment, and 3) stirring during the reaction on the formation of nanoscrolls are discussed on the basis of the following results. 1) Although a partial conversion into nanoscrolls is observed by heating $(C_{18})_2$DMA-Oct at 70 °C for 1 d in a Teflon-sealed autoclave (the SEM image is shown in Fig. S7), simple stirring at room temperature did not lead to the formation of nanoscrolls. This means that the treatment at higher temperature can be effective for the formation of nanoscrolls. 2) A simple heating of $(C_{18})_2$DMA-Oct at 70 °C for 1 d in heptane under stirring in a flask with a refluxing condenser did not afford nanoscrolls (Fig. S8a), which suggests the essential role of solvothermal treatment, or high pressure. 3) Also, nanoscrolls are not formed by the solvothermal treatment of $(C_{18})_2$DMA-Oct at 120 °C for 1 d in heptane *without* stirring (Fig. S8b). These results indicate that the use of a sealed container and stirring at high temperatures are necessary for scrolling. At normal temperature and pressure, $(C_{18})_2$DMABr cannot dissolve in heptane. Because both of the permittivity and viscosity of heptane at high pressures are higher than those at normal pressure,[23] the autogenous high pressure generated in the solvothermal environment contributes to an increase in the solubility of $(C_{18})_2$DMABr in heptane. In addition, stirring is effective in homogenizing viscous mixtures and hence contributes to an increased solubility.

On the basis of these results, we propose a mechanism for nanoscroll formation from layered octosilicates using solvothermal treatment. First of all, the intercalation of $(C_{18})_2$DMA cations into layered octosilicate can make the forces between the neighboring layers weaker to facilitate peeling and scrolling of the layers. $(C_{18})_2$DMA-Oct contains both $(C_{18})_2$DMA cations and a $(C_{18})_2$DMABr salt as described earlier. $(C_{18})_2$DMA cations electrostatically interact with SiO⁻

groups on the surfaces of the layers, while the $(C_{18})_2$DMABr salt participates in hydrophobic interactions with $(C_{18})_2$DMA cations. Because the outermost silicate surfaces also contain SiO^- groups, both $(C_{18})_2$DMA cations and the interacting $(C_{18})_2$DMABr salts should not only be in the interlayer but also on the outermost surfaces of the layers. The ease of desorption of $(C_{18})_2$DMABr salts is thought to be dependent on the location; those on the outermost surfaces should be desorbed more easily than those in the interlayer. Therefore, (i) $(C_{18})_2$DMABr salts on the outermost surfaces of layers are preferentially dissolved during solvothermal treatment. (ii) This preferential dissolution causes the formation of an asymmetric environment between the outermost layer with a lower density of $(C_{18})_2$DMABr and the underlying surfaces with a higher density of $(C_{18})_2$DMABr. (iii) A tensile force derived from the asymmetric structure and the shear flow generated by stirring promote the scrolling of layers (Scheme 2). According to this mechanism, the scrolling of layers occurs on the outermost surfaces of the particles before exfoliation, meaning that all the layers cannot scroll to form silicate nanoscrolls. In fact, we sometimes observed scrolls on particles (Fig. S5). Cooling and/or drying after solvothermal treatment may induce strain between the outermost and underlying surfaces to preface scrolling. The cooling speed after solvothermal treatment does not largely affect the formation of nanoscrolls, though we cannot deny the formation of nanoscrolls during the cooling process after solvothermal treatment or during the drying process.

The introduction of asymmetricity by the desorption of interlayer cointercalated salts is a new concept in the formation of scrolled layered materials, although we do not exactly understand the mechanism as yet. The method might be applicable to the generation of nanoscrolls from other layered materials as well. In particular, intercalation compounds with alkylammonium cations should be re-evaluated as precursors for nanoscrolls. We believe that the new nanoscrolling method proposed in this study will expand the chemistry of not only layered materials but also porous materials.

Conclusions

Silicate nanoscrolls with crystalline walls were obtained by the solvothermal treatment of $(C_{18})_2$DMA$^+$-intercalated layered octosilicate in heptane. Being different from natural layered silicates, such as chrysotile, hydrated halloysite, and artificially scrolled natural kaolinite, this is the first report on nanoscroll formation from synthetic layered silicate with crystalline walls to the best of our knowledge. The size of the tubular pores induced by the scrolling are in the range of boundary zone between meso- and macro-pores. Although the yield of silicate nanoscrolls is low, the nanoscrolls obtained can be regarded as nanoporous silica with crystalline walls and regularly arranged Si–OH groups on the inner and outer surfaces of nanoscrolled nanosheets. The nanoporous silica is a potentially promising material, because the pore walls can be modified in an ordered manner by virtue of the regularly arranged Si–OH

groups and the distance between the immobilized functional groups can be controlled. This will contribute to a deeper understanding of catalysis and chemical adsorption among other topics. This study is expected to motivate the re-evaluation of many layered silicates intercalated with long-chain alkyl ammonium cations as precursors for silicate nanoscrolls with crystalline walls.

Conflicts of interest

There are no conflicts of interest to declare.

Acknowledgements

Notes & References

†† Heptane was chosen as the nonpolar organic solvent on the basis of our preliminary studies using didecyldimethyl-ammonium cations. Nanoscrolls did not form for the cases of didecyldimethylammonium cations, though some delamination occurred, which suggests different interactions between dialkylammonium cations with different alkyl chain lengths and heptane in the solvothermal reaction for scrolling.

1 (a) R. Z. Ma, Y. Bando and T. Sasaki, *J. Phys. Chem. B*, 2004, **108**, 2115; (b) Z. C. Lai, Y. Chen, C. L. Tan, X. Zhang and H. Zhang, *Chem*, 2016, **1**, 59.

2 (a) L. M. Viculis, J. J. Mack and R. B. Kaner, *Science*, 2003, **299**, 1361; (b) M. V. Savoskin, V. N. Mochalin, A. P. Yaroshenko, N. I. Lazareva, T. E. Konstantinova, I. V. Barsukov and L. G. Prokofiev, *Carbon*, 2007, **45**, 2797; (c) X. Xie, L. Ju, X. F. Feng, Y. H. Sun, R. F. Zhou, K. Liu, S. S. Fan, Q. L. Li and K. L. Jiang, *Nano Lett.*, 2009, **9**, 2565.

3 X. L. Li, X. P. Hao, M. W. Zhao, Y. Z. Wu, J. X. Yang, Y. P. Tian and G. D. Qian, *Adv. Mater.*, 2013, **25**, 2200.

4 (a) Y. D. Li, X. L. Li, R. R. He, J. Zhu and Z. X. Deng, *J. Am. Chem. Soc.*, 2002, **124**, 1411; (b) C. Bouet, B. Mahler, B. Nadal, B. Abecassis, M. D. Tessier, S. Ithurria, X. Z. Xu and B. Dubertret, *Chem. Mater.*, 2013, **25**, 639; (c) R. B. Vasiliev, M. S. Sokolikova, A. G. Vitukhnovskii, S. A. Ambrozevich, A. S. Selyukov and V. S. Lebedev, *Quantum Electron.*, 2015, **45**, 853.

5 (a) R. Abe, K. Shinohara, A. Tanaka, M. Hara, J. N. Kondo and K. Domen, *Chem. Mater.*, 1997, **9**, 2179; (b) G. B. Saupe, C. C. Waraksa, H. N. Kim, Y. J. Han, D. M. Kaschak, D. M. Skinner and T. E. Mallouk, *Chem. Mater.*, 2000, **12**, 1556.

6 R. E. Schaak and T. E. Mallouk, *Chem. Mater.*, 2000, **12**, 3427.

7 (a) S. A. Corr, M. Grossman, J. D. Furman, B. C. Melot, A. K. Cheetham, K. R. Heier and R. Seshadri, *Chem. Mater.*, 2008, **20**, 6396; (b) A. V. Grigorieva, E. A. Goodilin, A. V. Anikina, I. V. Kollesnik and Y. D. Tretyakov, *Mendeleev Commun.*, 2008, **18**, 71; (c) J. Emmerich, E. Breynaert, C. E. A. Kirschhock and J. A. Martens, *Catal. Today*, 2012, **192**, 63.

8 K. Yada, *Acta. Crystallogr. A*, 1971, **A 27**, 659.

9 (a) B. Singh and I. D. R. Mackinnon, *Clays Clay Miner.*, 1996, **44**, 825; (b) J. E. F. C. Gardolinski and G. Lagaly, *Clay Miner.*, 2005, **40**, 547; (c) J. Matusik, A. Gawel, E. Bielanska, W. Osuch and K. Bahranowski, *Clays Clay Miner.*, 2009, **57**, 452; (d) Y. Kuroda, K. Ito, K. Itabashi and K. Kuroda, *Langmuir*, 2011, **27**, 2028.

10 (a) L. L. Ren, J. S. Hu, L. J. Wan and C. L. Bai, *Mater. Res. Bull.*, 2007, **42**, 571; (b) W. Lv, M. Du, W. Ye and Q. Zheng, *J. Mater. Chem. A*, 2015, **3**, 23395.

11 (a) M. A. Bizeto, W. A. Alves, C. A. S. Barbosa, A. M. D. C. Ferreira and V. R. L. Constantino, *Inorg. Chem.*, 2006, **45**, 6214; (b) R. Z. Ma, Y. Kobayashi, W. J. Youngblood and T. E. Mallouk, *J. Mater. Chem.*, 2008, **18**, 5982; (c) G. S. Machado, K. A. D. F. Castro, F. Wypych and S. Nakagaki, *J. Mol. Catal. A: Chem.*, 2008, **283**, 99; (d) K. Maeda, M. Eguchi, W. J. Youngblood and T. E. Mallouk, *Chem. Mater.*, 2008, **20**, 6770; (e) M. C. Sarahan, E. C. Carroll, M. Allen, D. S. Larsen, N. D. Browning and F. E. Osterloh, *J. Solid State Chem.*, 2008, **181**, 1678; (f) K. Maeda, M. Eguchi, S. H. A. Lee, W. J. Youngblood, H. Hata and T. E. Mallouk, *J. Phys. Chem. C*, 2009, **113**, 7962; (g) T. K. Townsend, E. M. Sabio, N. D. Browning and F. E. Osterloh, *ChemSusChem*, 2011, **4**, 185; (h) M. Kitano, E. Wada, K. Nakajima, S. Hayashi, S. Miyazaki, H. Kobayashi and M. Hara, *Chem. Mater.*, 2013, **25**, 385.

12 (a) L. Q. Mai, Q. L. Wei, Q. Y. An, X. C. Tian, Y. L. Zhao, X. Xu, L. Xu, L. Chang and Q. J. Zhang, *Adv. Mater.*, 2013, **25**, 2969; (b) F. Y. Zeng, Y. F. Kuang, G. Q. Liu, R. Liu, Z. Y. Huang, C. P. Fu and H. H. Zhou, *Nanoscale*, 2012, **4**, 3997; (c) K. M. Zhao, S. Q. Liu, Y. Z. Wu, K. Z. Lv, H. Yuan and Z. He, *Electrochim. Acta*, 2015, **174**, 1234.

13 P. Yuan, D. Tan and F. Annabi-Bergaya, *Applied Clay Science*, 2015, **112-113**, 75.

14 W. J. Roth, P. Nachtigall, R. E. Morris and J. Čejka, *Chem. Rev.*, 2014, **114**, 4807.

15 N. Takahashi and K. Kuroda, *J. Mater. Chem.*, 2011, **21**, 14336.

16 (a) M. E. Leonowicz, J. A. Lawton, S. L. Lawton and M. K. Rubin, *Science*, 1994, **264**, 1910; (b) L. Schreyeck, P. Caullet, J. C. Mougenel, J. L. Guth and B. Marler, *Microporous Mater.*, 1996, **6**, 259; (c) T. Ikeda, Y. Akiyama, Y. Oumi, A. Kawai and F. Mizukami, *Angew. Chem. Int. Ed.*, 2004, **43**, 4892; (d) S. Zanardi, A. Alberti, G. Cruciani, A. Corma, V. Fornes and M. Brunelli, *Angew. Chem. Int. Ed.*, 2004, **43**, 4933; (e) B. Marler, N. Stroter and H. Gies, *Microporous Mesoporous Mater.*, 2005, **83**, 201; (f) Y. X. Wang, H. Gies, B. Marler and U. Muller, *Chem. Mater.*, 2005, **17**, 43; (g) B. Marler, M. A. Camblor and H. Gies, *Microporous Mesoporous Mater.*, 2006, **90**, 87; (h) T. Moteki, W. Chaikittisilp, A. Shimojima and T. Okubo, *J. Am. Chem. Soc.*, 2008, **130**, 15780; (i) Y. Asakura, R. Takayama, T. Shibue and K. Kuroda, *Chem.-Eur. J.*, 2014, **20**, 1893; (j) Y. Asakura, S. Osada, N. Hosaka, T. Terasawa and K. Kuroda, *Dalton Trans.*, 2014, **43**, 10392; (k) J. E. Schmidt, D. Xie and M. E. Davis, *J. Mater. Chem. A*, 2015, **3**, 12890; (l) J. E. Schmidt, D. Xie and M. E. Davis, *Chem. Sci.*, 2015, **6**, 5955; (m) M. Koike, Y. Asakura, M. Sugihara, Y. Kuroda, H. Tsuzura, H. Wada, A. Shimojima and K. Kuroda, *Dalton Trans.*, 2017, **46**, 10232.

17 N. Takahashi, H. Tamura, D. Mochizuki, T. Kimura and K. Kuroda, *Langmuir*, 2007, **23**, 10765.

18 (a) E. Ruiz-Hitzky and J. M. Rojo, *Nature*, 1980, **287**, 28; (b) E. Ruiz-Hitzky, J. M. Rojo and G. Lagaly, *Colloid. Polym. Sci.*, 1985, **263**, 1025; (c) T. Yanagisawa, K. Kuroda and C. Kato, *React Solid*, 1988, **5**, 167; (d) M. Ogawa, S. Okutomo and K. Kuroda, *J. Am. Chem. Soc.*, 1998, **120**, 7361; (e) A. Shimojima, D. Mochizuki and K. Kuroda, *Chem. Mater.*, 2001, **13**, 3603; (f) D. Mochizuki, A. Shimojima and K. Kuroda, *J. Am. Chem. Soc.*, 2002, **124**, 12082; (g) D. Mochizuki, A. Shimojima, T. Imagawa and K. Kuroda, *J. Am. Chem. Soc.*, 2005, **127**, 7183;

(h) D. Mochizuki, S. Kowata and K. Kuroda, *Chem. Mater.*, 2006, **18**, 5223; (i) Y. Ide, S. Iwasaki and M. Ogawa, *Langmuir*, 2011, **27**, 2522; (j) Y. Asakura, Y. Matsuo, N. Takahashi and K. Kuroda, *Bull. Chem. Soc. Jpn.*, 2011, **84**, 968; (k) Y. Asakura, Y. Sakamoto and K. Kuroda, *Chem. Mater.*, 2014, **26**, 3796.

19 (a) Y. Mitamura, Y. Komori, S. Hayashi, Y. Sugahara and K. Kuroda, *Chem. Mater.*, 2001, **13**, 3747; (b) S. Kiba, T. Itagaki, T. Nakato and K. Kuroda, *J. Mater. Chem.*, 2010, **20**, 3202.

20 S. Osada, A. Iribe and K. Kuroda, *Chem. Lett.*, 2013, **42**, 80.

21 S. Vortmann, J. Rius, S. Siegmann and H. Gies, *J. Phys. Chem. B*, 1997, **101**, 1292.

22 G. H. Du, Q. Chen, Y. Yu, S. Zhang, W. Z. Zhou and L. M. Peng, *J. Mater. Chem.*, 2004, **14**, 1437.

23 (a) Y. J. Shen, A. R. H. Goodwin and L. Pirolli, *J. Chem. Eng. Data*, 2013, **58**, 2131; (b) E. Kiran and Y. L. Sen, *Int. J. Thermophys.*, 1992, **13**, 411.

24 C. Izutani, D. Fukagawa, M. Miyasita, M. Ito, N. Sugimura, R. Aoyama, T. Gotoh, T. Shibue, Y. Igarashi and H. Oshio, *J. Chem. Educ.*, 2016, **93**, 1667.

Table of Contents
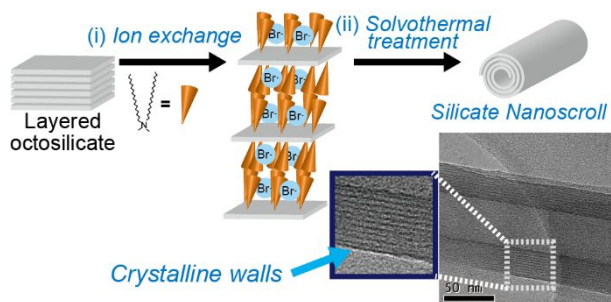
Silicate nanoscrolls with crystalline walls were prepared by intercalation of layered octosilicate with organoammonium ions and the subsequent solvothermal treatment.